Novel Ion Specificity of a Carboxylate Cluster Mg(II) Binding Site: Strong Charge Selectivity and Weak Size Selectivity†

James V. Needham, Theodore Y. Chen, and Joseph J. Falke*

Department of Chemistry and Biochemistry, University of Colorado, Boulder, Colorado 80309-0215

Received November 16, 1992

ABSTRACT: Carboxylate cluster Mg(II) binding sites consist of a cluster of side-chain carboxylates, typically 3–4 in number, partially buried in a shallow cleft on the surface of a Mg(II) binding protein. Such clusters are often found in the active sites of enzymes catalyzing phosphochemistry. An example is the phosphosignaling protein CheY of the *Escherichia coli* chemotaxis pathway, which binds Mg(II) via a cluster of three carboxylates at its phosphorylation site. The present study quantitates both the ion charge and size specificity of the CheY site by measuring the dissociation constants of metal ions from groups Ia, IIa, IIIa, and the lanthanides; these spherical cations provide a range of substrates with incrementally varying charge and radius. The site binds divalent and trivalent cations, but it effectively excludes monovalent cations, including the physiological ions Na(I) and K(I). This charge specificity is in contrast to the site's remarkable lack of size specificity: divalent and trivalent cations exhibit affinities which are essentially independent of radius. It is revealing to compare the ion specificity of the Mg(II) site with the previously characterized specificity of the EF-hand class of Ca(II) sites commonly found in Ca(II) signaling proteins. The Mg(II) and Ca(II) sites exhibit similar charge selectivity, but the Ca(II) site is highly size-selective, preferring divalent and trivalent ions with radii similar to that of Ca(II). A structural comparison of the Mg(II) and Ca(II) sites suggests that their different size specificities stem from fundamentally different coordination schemes: the Ca(II) site surrounds the bound ion with a pentagonal bipyramidal array of seven protein oxygens, thereby fixing the coordination number and controlling the radius of the substrate cavity. In contrast, the adjustable nature of the Mg(II) site is proposed to stem from its use of solvent oxygens to coordinate one hemisphere of the bound ion: this solvent shell can easily vary its coordination number and radius to accommodate substrate ions of different size.

Bound Mg(II) ion is an essential active-site component of the numerous phosphoenzymes catalyzing various phosphate chemistries, including polymerases, nucleases, and phosphotransfer proteins such as kinases and phosphatases. Moreover, recent evidence suggests that intracellular Mg(II) functions as a regulatory ion in eukaryotic systems: transmembrane Mg(II) fluxes triggered by hormonal stimulation have been observed in specific cell types, and in at least one case the trigger is dependent upon protein kinase C signaling (Romani et al., 1992; Gonzales, 1992; Zhang et al., 1992; Murphy et al., 1991; Preston, 1990; Romani & Scarpa, 1990). The existence of Mg(II) regulation in turn requires the existence of Mg(II) binding sites with metal ion affinities and specificities appropriate for activation in the physiological ionic environment. Although Mg(II)-regulated proteins have not yet been identified, the phosphochemistry enzymes themselves are likely candidates.

Phosphoenzymes of known structure often exhibit a Mg(II) binding motif termed the carboxylate cluster site. Each carboxylate cluster site consists of 3–4 side-chain carboxylates grouped in a solvent-exposed cleft. This motif is widely observed in metabolic phosphotransfer enzymes (Kim & Wyckoff, 1991; Lebioda & Stec, 1991; Ke et al., 1990; Knight et al., 1990; Shirakihara & Evans, 1988), nucleases (Katayanagi et al., 1992; Jou & Cowan, 1991; Davies et al., 1991; Wang et al., 1990; Derbyshire et al., 1988), and phosphoregulated signaling proteins (Stock et al., 1989; Volz & Matsumura, 1991; Stock et al., 1992). Such proteins use Mg(II) ion for phospho-substrate binding, catalysis, or both; however, key features of their metal binding characteristics remain undetermined. For example, it is known that Mn(II) and certain other divalent cations can typically be substituted for Mg(II) (Kim & Wyckoff, 1991; Davies et al., 1991; Lukat et al., 1990; Katayanage et al., 1990), yet no systematic study of the ion specificity of a carboxylate cluster site has been described. Of particular interest is whether these sites can distinguish metal ions on the basis of ionic radius and charge, in analogy with highly specific Ca(II) sites. Alternatively, Mg(II) sites might be relatively nonselective, since Mg(II) is ≥100-fold more abundant than other divalent metal ions in cellular systems.

The present study quantitates the ion specificity of the carboxylate cluster site of CheY, a phosphorylation-activated signaling protein of the bacterial chemotaxis pathway [reviewed by Parkinson and Kofoid (1992), Stock et al. (1992) and Bourret et al. (1991)]. Mg(II) binding to this carboxylate cluster plays a central functional role by catalyzing the phosphorylation and dephosphorylation of Asp57, one of three carboxylates in the cluster. Similar or identical carboxylate clusters are ubiquitous in the prokaryotic response regulators, a class of phospho-activated signaling proteins evolutionarily related to CheY, which control cellular responses to a wide variety of intra- and extracellular stimuli (Parkinson & Kofoid, 1992; Bourret et al., 1991; Stock et al., 1991).

The CheY Mg(II) site is illustrated in Figure 1, where Asp12, Asp13, and Asp57 comprise the carboxylate cluster (Stock et al., 1989; Volz & Matsumura, 1991). The 1.7-Å resolution structure of the Mg(II)-occupied site (Stock et al., 1992) reveals that the bound ion is coordinated by the monodentate side-chain carboxylates of Asp13 and Asp57, the backbone carbonyl of Asn59, and three water molecules,

† This work was supported by NIH Grant R01-GM48203.

* Corresponding author.

0006-2960/93/0432-3363$04.00/0

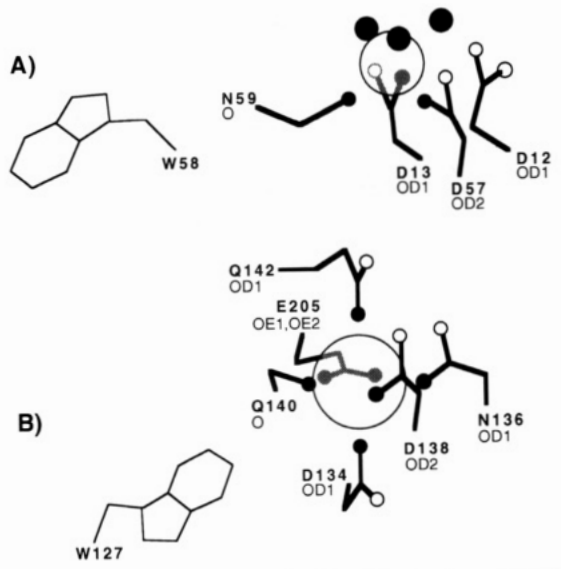

FIGURE 1: Structures of the model carboxylate cluster and EF-hand sites. (A) Carboxylate cluster Mg(II) site of *E. coli* CheY, adapted from the 1.7-Å structure of the Mg(II)-occupied site (Stock et al., 1992). Bound Mg(II) (large sphere) is held by three protein oxygens (small filled circles) coordinating the lower hemisphere of the metal ion and by three solvent oxygens (larger filled circles) coordinating the upper hemisphere. (B) EF-hand-like Ca(II) binding site of the *E. coli* D-galactose chemosensory receptor, determined to 1.9-Å resolution (Vyas et al., 1987). The bound Ca(II) ion (large sphere) is completely surrounded by a pentagonal bipyramidal array of seven protein coordinating oxygens (filled circles).

one of which is stabilized by outer-sphere coordination to Asp12. An interesting feature of the coordination structure is that one hemisphere of the bound ion is coordinated by three protein oxygens, while the other hemisphere is coordinated by three solvent molecules at the protein surface.

In order to quantitate the metal ion affinity and specificity of the CheY Mg(II) site, we have determined the binding affinities for the cations of groups Ia, IIa, IIIa, and the lanthanides, which can be treated as simple ionic spheres of different charge and radius: these ions lack preference for specific coordination geometry due to their filled outer electronic subshells (Snyder et al., 1990). As previously shown (Lukat et al., 1990), ion binding can be measured using the intrinsic fluorescence of the Trp58 indole ring located within 8 Å of the bound ion (Figure 1). The present study also utilizes a competitive binding assay which monitors the fluorescence of Tb(III) bound in the site. The results reveal that the site possesses a unique ion specificity which, in comparison with a model EF-hand Ca(II) site, exhibits similar ion charge selectivity but a novel lack of size selectivity. Such information illuminates key features of the mechanisms underlying ion specificity, both for carboxylate cluster Mg(II) sites and for EF-hand Ca(II) sites.

MATERIALS AND METHODS

Reagents. Metal ion stocks were prepared immediately before use from the highest commercially available grade of the chloride salt. The KCl used to approximate physiological ionic strength was specially purified to remove multivalent cations [ionic strength adjuster for Ca(II) electrodes, Orion Instruments, Inc.]. Solvent H_2O was deionized and then glass-distilled, and plasticware was used rather than glassware to avoid metal contaminants. When glassware was required, for example, in fluorescence titrations utilizing quartz cuvettes, extensive rinsing with 100 mM EDTA and H_2O was undertaken prior to use.

Purified E. coli CheY Protein. Plasmid pRBB40 (Bourret et al., 1990), which contains the *cheY* gene under control of the *trp* promoter, was expressed in an *Escherichia coli* strain gutted for CheY and other chemotaxis proteins (RBB455 = HCB440 *aux*(*phe43A*)::Tn10) (Wolfe et al., 1988). Expression and isolation were carried out as previously described (Hess et al., 1991), with the following modifications. Cell growth was at 37 °C in Luria broth (LB) containing 0.1 mg/mL ampicillin until cell density reached $OD_{600} = 1.0$, at which point 0.1 mg/mL 3-β-indole acrylic acid was added to induce expression. After growth, cells were isolated by centrifugation and washed in TEDG buffer: 50 mM Tris, pH 7.5 w/HCl, 1 mM EDTA, 2 mM DTT, and 10% (v/v) glycerol. Cells were lysed by French press, and then cell fragments were removed by ultracentrifugation and filtration through a 0.45-μm syringe filter. The resulting filtrate was applied to an Affi-Gel Blue column (Bio-Rad) equilibrated with TEDG. CheY bound tightly during washing, first with TEDG and then with TEDG containing 0.05 M NaCl. Elution was with TEDG containing a linear 0.05–1.5 M NaCl gradient. The CheY fractions were pooled, concentrated by ultrafiltration (Amicon, YM3 membrane), and then further purified by FPLC with a Superdex 75 gel-filtration column (Pharmacia) equilibrated with TEDG containing 0.75 M NaCl. After concentration by ultrafiltration to 100–200 μM, the protein was dialyzed three times against 300–500 volumes of titration buffer: 25 mM triethanolamine, pH 7.0 w/HCl, and 100 mM KCl. The resulting protein was quick-frozen in liquid N_2 and stored at –20 °C until use.

Fluorescence Determination of Metal Ion Dissociation Constants. Two types of fluorescence titrations were used to monitor metal ion binding. The first monitored the quenching of Trp58 intrinsic fluorescence upon metal ion binding (Lukat et al., 1990); spectral parameters were ex = 282 nm, em = 348 nm, and bandwidths = 4 and 8 nm, respectively. The second detected the fluorescence of Tb(III) bound in the site, which was competitively displaced by titration with a second metal of interest (Snyder et al., 1990; Brittain et al., 1979; Horrocks et al., 1976; Falke et al., 1991); spectral parameters were ex = 292 nm, em = 546 nm, and bandwidth = 8 nm. All fluorescence titrations were carried out at 20 °C using an SLM 48000S spectrofluorometer.

For both methods, nonlinear least-squares analysis was used to determine the dissociation constant (K_D) from the untransformed binding titration:

$$F/F_0 = 1 - C[M]/([M] + K_D) \quad (1)$$

where F and F_0 are the fluorescence intensities in the presence and absence of metal ion, respectively, [M] is the free metal ion concentration (Falke et al., 1991), and C is the fraction of total fluorescence quenched at saturating metal concentrations. When the Tb(III) displacement assay is used, eq 1 yields the apparent dissociaton constant (K_D^{app}), which must be corrected for the presence of competing Tb(III), thereby yielding the true dissociation constant:

$$K_D = K_D^{app}/(1 + [Tb(III)]/K_{Tb}) \quad (2)$$

where K_{Tb} is the dissociation constant for Tb(III). Finally the dissociation constant provided by eq 1 or 2 is converted to a binding free energy:

$$\Delta G^0_B = RT \ln K_D \quad (3)$$

namely, the free energy of binding for a 1 M standard state concentration.

Calculations involving eqs 1 and 2 utilized the molar concentration of the free ion, rather than its activity in the titration buffer. This approximation is valid because the relevant ionic conditions yield activity coefficients of the same order as unity, ranging from $0.4 \leq \gamma \leq 1.0$ for all metal ions included in the study (Harned & Owen, 1954). Thus activity corrections would decrease the ΔG^0_B values by no more than 0.2 kcal mol^{-1}.

RESULTS

Approach. The incrementally varying metal cations of groups Ia, IIa, and IIIa and the lanthanides provide the substrates needed to quantitative both the ionic size and charge selectivity of the carboxylate cluster. The charges of these metal ions range from +1 to +3, and their radii range from 0.72 to 1.52 Å.

In order to determine the dissociation constant for each metal ion, two fluorescence methods were utilized. The first relied on direct quenching of Trp58 fluorescence upon metal binding (Lukat, 1990), which in the case of trivalent group IIIa or lanthanide ion binding reduced the Trp58 quantum yield 30–50%. In contrast, bound ions of groups Ia and IIa yielded at most 0–20% quenching; thus for these monovalent and divalent ions a more sensitive assay was required. This second method employed the fluorescent lanthanide Tb(III) as a probe ion (Snyder et al., 1990; Brittain et al., 1979; Horrocks et al., 1976; Falke et al., 1991). Tb(III) bound in the cluster was excited by nonradiative excitation transfer from Trp58 and then the resulting bound Tb(III) fluorescence was monitored, enabling detection of the binding of a competing metal ion via its displacement of bound Tb(III) fluorescence.

The fluorescence titration data were analyzed using eqs 1–3, yielding for each metal ion a dissociation constant and binding free energy describing the equilibrium

$$\mathrm{R{\cdot}(H_2O)}_m + \mathrm{M{\cdot}(H_2O)}_j \underset{K_D}{\overset{\Delta G^0_B}{\rightleftharpoons}} \mathrm{R^*{\cdot}M{\cdot}(H_2O)}_k + (m + j - k)\mathrm{H_2O} \quad (4)$$

Here the site R and metal ion M are partially dehydrated upon binding, and the site undergoes a conformational change to yield R*. A comparison of the binding equilibria of different metal ions is facilitated by the fact that the hydrated empty site R, which is identical for all substrates, can be ignored. It follows that only two factors contribute to the affinity differences observed between nonidentical metal ions: (1) a difference in their metal ion dehydration free energies and (2) a difference in the free energy of binding of the partially dehydrated metal ions to the hydrated site.

Metal Ion Affinity and Specificity of the Carboxylate Cluster Site. Table I summarizes the ionic radii, dissociation constants, and binding free energies of the chosen metal ions. The observed dissociation constant for Mg(II) [K_D = 1.0 ± 0.2 mM; Table I and Lukat et al. (1990)] is the same order of magnitude as intracellular Mg(II) activities (Williams, 1980; Tsai et al., 1987), demonstrating that the Mg(II) affinity of carboxylate cluster sites can be tuned to a value appropriate for Mg(II) regulation.

The charge specificity of the site is revealed by its different affinities for monovalent, divalent, and trivalent cations (Table I). Monovalent metal ions are essentially excluded from the site, exhibiting dissociation constants in the range $K_D \geq 0.2$ M. Divalent and trivalent metal ions exhibit measurable affinities, ranging between 0.4 and 1 mM for divalent ions, and between 1 and 10 μM for trivalent ions. Thus each metal ion positive charge increases the metal affinity by 2–3 orders of magnitude.

Table I: Dissociation Constants for Metal Ion Binding to the CheY Mg(II) Site

ion	effective ionic radius[a] (Å) CN = 6	preferred CN	K_D ± 1 SD[b] (M)	$\Delta G^\circ_{binding}$ (kcal/mol)	assay
group Ia					
Li(I)	0.76	(6)[c] 0.76	>0.2	>–0.9	e
Na(I)	1.02	(6) 1.02	>0.2	>–0.9	e
K(I)	1.38	(8) 1.51	>0.4	>–0.5	e
Rb(I)	1.52	(12) 1.72	>0.2	>–0.9	e
group IIa					
Mg(II)	0.72	(6) 0.72	$(1.0 \pm 0.2) \times 10^{-3}$	–4.0	d,e
Ca(II)	1.00	(7)[c] 1.06	$(0.4 \pm 0.1) \times 10^{-3}$	–4.5	e
Sr(II)	1.18	(8)[c] 1.26	$(0.8 \pm 0.2) \times 10^{-3}$	–4.2	e
Ba(II)	1.35	(8) 1.42	$(0.6 \pm 0.2) \times 10^{-3}$	–4.3	e
group IIIa					
Sc(III)	0.74	(6) 0.74	$(6.3 \pm 1.7) \times 10^{-6}$	–7.0	d
Y(III)	0.90	(8) 1.02	$(4.8 \pm 0.7) \times 10^{-6}$	–7.1	d
La(III)	1.03	(8) 1.16	$(2.5 \pm 0.9) \times 10^{-6}$	–7.5	d
lanthanides					
Lu(III)	0.86	(6) 0.86	$(7.5 \pm 0.2) \times 10^{-6}$	–6.9	d,e
Yb(III)	0.87	(6)[c] 0.87	$(10 \pm 4) \times 10^{-6}$	–6.7	d
Tb(III)	0.88	(8) 0.99	$(12 \pm 1) \times 10^{-6}$	–6.6	d
Er(III)	0.89	(8) 1.00	$(5.6 \pm 1.1) \times 10^{-6}$	–7.0	d
Ho(III)	0.90	(8) 1.01	$(11 \pm 2) \times 10^{-6}$	–6.7	d
Dy(III)	0.91	(8) 1.03	$(4.5 \pm 1.4) \times 10^{-6}$	–7.2	d,e
Tb(III)	0.92	(8) 1.04	$(3.1 \pm 1.3) \times 10^{-6}$	–7.4	d
Gd(III)	0.94	(7) 1.00	$(1.9 \pm 0.2) \times 10^{-6}$	–7.7	d
Eu(III)	0.95	(8)[c] 1.07	$(3.5 \pm 2.2) \times 10^{-6}$	–7.3	d
Sm(III)	0.96	(9) 1.13	$(1.8 \pm 0.2) \times 10^{-6}$	–7.7	d
Nd(III)	0.98	(8) 1.11	$(1.8 \pm 0.3) \times 10^{-6}$	–7.7	d
Pr(III)	0.99	(9) 1.18	$(3.7 \pm 0.9) \times 10^{-6}$	–7.3	d
Ce(III)	1.01	(9)[c] 1.20	$(2.2 \pm 0.4) \times 10^{-6}$	–7.6	d

[a] Effective ionic radii for the indicated coordination number (Shannon, 1976). [b] Dissociation constants were determined as described in Materials and Methods for the following conditions: 1 μM CheY, 100 mM KCl, and 25 mM triethanolamine, pH 7.0, and 20 °C. Due to the low affinities of monovalent ions, only their lower limit K_D was determined. [c] The coordination number observed most frequently in small molecule complexes is given in parentheses (Shannon, 1976); the indicated metals exhibit two or more equally preferred coordination numbers. [d] Fluorescence quenching of Trp58. [e] Competitive displacement of bound Tb(III) monitored by nonradiative fluorescence energy transfer.

In contrast to its charge specificity, the carboxylate cluster site exhibits a striking lack of size specificity. Figure 2A plots the binding free energies of divalent and trivalent metal ions against their ionic radii. No stable free energy minimum is observed, indicating that the site prefers no specific ion size. Instead the free energy curves are relatively flat with a small negative slope of magnitude ≤2 kcal/mol·Å. The sign of the slope suggests that large ions are bound with slightly higher affinity, presumably due to the greater ease of dehydration of large ions, since dehydration free energy is an inverse function of metal ion radius (Rashin & Honig, 1985).

Comparison of the Carboxylate Cluster Site to an EF-Hand-like Ca(II) Site. It is revealing to compare the ion specificity of the Mg(II) site with that of a representative Ca(II) site: for example, the EF-hand-like Ca(II) site of the *E. coli* D-galactose chemosensory receptor (Vyas et al., 1987). Previous studies have fully characterized the ion specificity of this site; binding free energy curves are plotted in Figure 2B for both divalent and trivalent ions (Snyder et al., 1990). Like the carboxylate cluster site, the Ca(II) site essentially excludes monovalent cations but binds divalent and trivalent cations. However, the Ca(II) site exhibits a strong preference for a metal ion of specific size, yielding a binding free energy

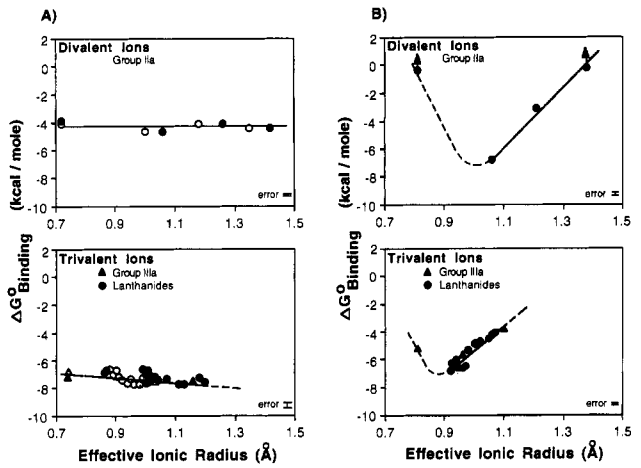

FIGURE 2: Free energies of metal ion binding to (A) the CheY Mg(II) site and (B) the D-galactose chemoreceptor Ca(II) site, as a function of effective ionic radius. Binding free energies were measured by fluorescence titrations carried out as in (A) Materials and Methods or (B) Snyder et al. (1990). Effective ionic radii were determined as follows. For the Mg(II) site, Table I lists the effective ionic radius for the two possible extremes of coordination numbers (CN) for each ion (Shannon, 1976): the minimum radius (CN = 6, open symbols) holds if the coordination is optimized for Mg(II), while the maximum radius (preferred CN, closed symbols) holds if the solvent coordination varies to maintain the preferred coordination number for each ion. For the Ca(II) site, effective ionic radii are those for a fixed CN = 7 (Synder et al., 1990; Shannon, 1976). Indicated in each plot is the maximum error of the data set, determined from binding free energies for $K_D \pm 1$ standard deviation. Titration samples contained the following components: (A) 1 μM CheY, 100 mM KCl, and 25 mM triethanolamine, pH 7.0; (B) 2.5 μM D-galactose chemosensory receptor, 100 mM KCl, and 10 mM PIPES, pH 6.0.

well approximately 7 kcal mol^{-1} deep with an optimal radius centered near Ca(II). The slope of this free energy curve ranges up to 25 kcal $(mol \cdot Å)^{-1}$, a slope ≥10-fold steeper than the Mg(II) site. Similar selectivities are exhibited by other EF-hand Ca(II) binding sites, particularly those of the cryptand class including the N-terminal sites of the parvalbumin family (Cavé et al., 1979; Corson et al., 1983; Chao et al., 1984). At least for ions above the optimal radius, this strong size selectivity must stem from constraints within the Ca(II) site rather than from differences in metal ion dehydration (the latter would yield a slope of opposite sign because large ions are more easily dehydrated).

DISCUSSION

The observed ion binding characteristics of the model Mg(II) and Ca(II) sites (Figure 2), together with the available structural information for these sites (Figure 1), suggest key structural features likely to control their respective metal ion selectivities. The similarity in charge selectivity is correlated with the observation that both sites possess three acidic residues. The negative charges of these carboxylates, together with the partial negative charges of other inner- and outer-sphere oxygens in each site, are likely to generate strong repulsive electrostatic interactions within the coordinating array. Such a picture suggests that substrate cations must possess sufficient positive charge to stabilize the folded, deprotonated structure of the occupied site, thereby explaining why monovalent ions are excluded while divalent and trivalent ions are bound (Snyder et al., 1990; Falke et al., 1991).

The different size selectivities of the sites are correlated with their different coordination environments. The Ca(II) site provides a fixed coordination number of 7 (Strynadka & James, 1989), which is compatible with the weak preference of Ca(II) for 7-fold coordination, while at the same time disfavoring ions that prefer other coordination numbers including the smaller Mg(II) (6-fold) and the larger Sr(II) (8-fold) (Shannon, 1976). In addition, the Ca(II) site provides an ion binding cavity fully surrounded by the coordinating protein oxygens: studies of engineered sites indicate that the positions of these oxygens are constrained so that expansion of the cavity requires work (Falke et al., 1991). The Mg(II) site, in contrast, can neither fix the coordination number nor provide a constrained ion cavity because one hemisphere of the bound metal is coordinated by solvent. In such a site, ions of different sizes are free to optimize their coordination by varying the number and spacing of inner-sphere solvent oxygens, thereby requiring little or no rearrangement of the protein to accommodate large ions.

Finally, the ion specificities observed for these Mg(II) and Ca(II) sites are compatible with the ionic physiologies of typical prokaryotic and eukaryotic cells. K(I) and Na(I) are the most abundant intracellular metal ions; thus Mg(II) and Ca(II) sites have evolved to exclude monovalent cations. Mg(II) is the most abundant divalent cation, exhibiting intracellular activities at least 2 orders of magnitude greater than other multivalent metal ions including Ca(II); thus Mg(II) sites need not exclude such ions. In contrast, Ca(II) binding sites, particularly signaling sites which must remain empty until a Ca(II) burst, exhibit the strong size selectivity required for exclusion of Mg(II). Trivalent cations are essentially nonexistent in the cellular environment; thus neither Mg(II) nor Ca(II) sites have evolved the ability to reject them. Overall, the current results provide further impetus for studies of the involvement of carboxylate cluster sites in Mg(II) regulation.

ACKNOWLEDGMENT

We thank M. I. Simon and R. B. Bourret for providing the CheY expression system, K. Volz for the coordinates of CheY, and F. A. Quiocho for coordinates of the D-galactose chemosensory receptor.

REFERENCES

Bourret, R. B., Hess, J. F., & Simon, M. I. (1990) *Proc. Natl. Acad. Sci. U.S.A. 87*, 41–45.
Bourret, R. B., Borkovitch, K. A., & Simon, M. I. (1991) *Annu. Rev. Biochem. 60*, 401–441.
Brittain, H. G., Richardson, F. S., & Martin, R. B. (1979) *J. Am. Chem. Soc. 98*, 8255–8260.
Cavé, A., Daurer, M. F., Parello, J., Saint-Yves, A., & Sempéré, R. (1979) *Biochimie 61*, 755–765.
Chao, S. H., et al. (1984) *Mol. Pharmacol. 26*, 8255–8260.
Corson, D. C., Williams, T. C., & Sykes, B. D. (1983) *Biochemistry 22*, 5882–5889.
Davies, J. F., Hostomska, Z., Hostomsky, Z., Jordan, J. R., & Mattews, D. A. (1991) *Science 252*, 88–95.
Derbyshire, V., Freemont, P. S., Sanderman, M. S., Beese, L., Friedman, J. M., Joyce, C. M., & Steitz, T. A. (1988) *Science 240*, 199–203.
Falke, J. J., Snyder, E. E., Thatcher, K. S., & Voertler, C. S. (1991) *Biochemistry 30*, 8690–8697.
Gonzales, R. A. (1992) *J. Neurochem. 58*, 579–586.
Harned, H. S., & Owen, B. B. (1954) *Physical Chemistry of Electrolytic Solutions*, Reinhold Publishing Corp., New York.
Hess, J. F., Bourret, R. B., & Simon, M. I. (1991) *Methods Enzymol. 200*, 188–204.
Horrocks, W. DeW., Jr., & Albin, B. (1976) *Prog. Inorg. Chem. 31*, 1–104.
Jou, R. W., & Cowan, J. A. (1991) *J. Am. Chem. Soc. 113*, 6685–6686.

Katayanage, K., Miyagawa, M., Matsushima, M., Ishikawa, M., Kanaya, S., Ikehara, M., Matsuzaki, T., & Morikawa, K. (1990) *Nature 347*, 306–309.
Katayanagi, K., et al., (1992) *J. Mol. Biol. 223*, 1029–1052.
Ke, H., Zhang, Y., & Lipscomb, W. N. (1990) *Proc. Natl. Acad. Sci. U.S.A. 87*, 5243–5247.
Kim, E. E., & Wyckoff, H. W. (1991) *J. Mol. Biol. 218*, 449–464.
Knight, S., Anderson, I., & Brändén, C.-I. (1990) *J. Mol. Biol. 215*, 113–160.
Lebioda, L., & Stec, B. (1991) *Biochemistry 30*, 2817–2822.
Lukat, G. S., Stock, A. M., & Stock, J. B. (1990) *Biochemistry 29*, 5436–5442.
Murphy, E., Freudenrich, C. C., & Lieberman, M. (1991) *Annu. Rev. Physiol. 53*, 273–287.
Parkinson, J. S., & Kofoid, E. C. (1992) *Ann. Rev. Genet.* (in press).
Preston, R. R. (1990) *Science 250*, 285–288.
Rashin, A. A., & Honig, B. (1985) *J. Phys. Chem. 89*, 5588–5593.
Romani, A., & Scarpa, A. (1990) *Nature 346*, 841–843.
Romani, A., Marfella, C., & Scarpa, A. (1992) *FEBS Lett. 296*, 135–140.
Shannon, R. D. (1976) *Acta Crystallogr. A32*, 751–767.
Shirakihara, Y., & Evans, P. R. (1988) *J. Mol. Biol. 204*, 973–994.
Snyder, E. E., Buoscio, B. B., & Falke, J. J. (1990) *Biochemistry 29*, 3937–3943.
Stock, A. M., Mottonen, J. M., Stock, J. B., & Schutt, C. E. (1989) *Nature 337*, 745–749.
Stock, J. B., Lukat, G. S., & Stock, A. M. (1991) *Annu. Rev. Biophys. Biophys. Chem. 20*, 109–136.
Stock, J. B., Surette, M. G., McCleary, W. R., & Stock, A. M. (1992) *J. Biol. Chem. 267*, 19753–19756.
Strynadka, N. C., & James, M. N. G. (1989) *Annu. Rev. Biochem. 58*, 951–998.
Tsai, M.-D., Drakenberg, T., Thulin, E., & Forsén, S. (1987) *Biochemistry 26*, 3635–3643.
Volz, K., & Matsumura, P. (1991) *J. Biol. Chem. 266*, 15511–15519.
Vyas, N. K., Vyas, M. N., & Quiocho, F. A. (1987) *Nature 327*, 635–638.
Wang, W., Hendrickson, W. A., Crouch, R. J., & Satow, Y. (1990) *Science 249*, 1398–1405.
Williams, R. J. P. (1980) in *Calcium Binding Proteins: Structure and Function* (Siegel, F. L., et al., Eds.) pp 3–10, Elsevier, Amsterdam.
Wolfe, A. J., Conley, M. P., & Berg, H. C. (1988) *Proc. Natl. Acad. Sci. U.S.A. 85*, 6711–6715.
Zhang, A., Cheng, T., & Altura, B. M. (1992) *Biochim. Biophys. Acta 1134*, 25–29.